Electrically tunable near-field radiative heat transfer via ferroelectric materials

Citation: Huang, Yi, Svetlana V. Boriskina, and Gang Chen. “Electrically Tunable Near-Field Radiative Heat Transfer via Ferroelectric Materials.” Appl. Phys. Lett. 105, no. 24 (December 15, 2014): 244102.

Published Version: http://dx.doi.org/10.1063/1.4904456

Publisher: American Institute of Physics (AIP)

Permanent Link: http://hdl.handle.net/1721.1/96916

Version: Author's final manuscript: final author’s manuscript post peer review, without publisher’s formatting or copy editing

Electrically-Tunable Near-field Radiative Heat Transfer via Ferroelectric Materials

Yi Huang[1], Svetlana V. Boriskina[1], and Gang Chen[1†]

[1]*Department of Mechanical Engineering, Massachusetts Institute of Technology, Cambridge, 02139 Massachusetts, USA*

ABSTRACT

We explore ways to actively control near-field radiative heat transfer between two surfaces that relies on electrical tuning of phonon modes of ferroelectric materials. Ferroelectrics are widely used for tunable electrical devices such as capacitors and memory devices; however, their tunable properties have not yet been examined for heat transfer applications. We show via simulations that radiative heat transfer between two ferroelectric materials can be enhanced by over two orders of magnitude over the blackbody limit in the near field, and can be tuned as much as 16.5% by modulating the coupling between surface phonon polariton modes at the two surfaces via varying external electric fields. We then discuss how to maximize the modulation contrast for tunable thermal devices using the studied mechanism.

Keywords: Ferroelectrics, Near-field Radiation, Tunable Heat Transfer, Energy Transport, Surface Phonon Polaritons

It has already been demonstrated both experimentally and theoretically that thermal emission and radiative heat exchange between hot and cold surfaces is modified dramatically when the surfaces are brought into a close proximity [1 – 11]. At separation distances smaller than the dominant wavelength of thermal radiation, the radiative heat flux has been demonstrated to be orders of magnitude higher than the blackbody limit predicted by the Planck and the Stefan-Boltzmann laws [3 - 9]. One major reason for such enhancement is that photons can couple resonantly with optical phonons in polar materials at the material surface to form surface phonon polariton (SPP) waves [3 – 11], which

† To whom correspondence should be addressed
gchen2@mit.edu

exponentially decay from the surface but can tunnel through the vacuum gap between hot and cold surfaces when the gap size is small [3 - 11]. Several calculations and experiments have shown that near-field radiative heat flux can be controlled by modifying the geometries of thermal emitters and absorbers [13 - 19] as well as by using materials with externally variable optical properties, such as vanadium dioxide that undergoes a metal-insulator transition [20, 22, 23], semiconductors with different levels of doping [25, 26], modulation of graphene optical properties via electrostatic gating [27, 28], dynamic magnetoelectric coupling in metamaterials [29], and modulation of intersubband transition rates in a quantum cascade laser [30]. In this paper, we investigate an approach to actively control radiative heat flux via applying external electric field that causes the softening (i.e. decrease in frequency) and hardening (i.e. increase in frequency) of transverse optical (TO) phonon mode in ferroelectric materials [32, 34 - 38].

Tunability of the TO phonon mode in perovskite-structure ferroelectric materials stems from the material structure instability [31, 32, 34 - 38]. One unique property of ferroelectrics is that its static dielectric constant can be modulated by external dc electric field and temperature by inducing crystal structure changes within the material [31], which is most effective near the Curie temperature (i.e. phase transition temperature between ferroelectric and paraelectric phases) [12]. The static dielectric constants in polar materials are related to their TO phonon frequencies through the Lydanne-Sachs-Teller relation [12]. Since surface phonon polaritons exist near optical phonon frequencies of the material, external dc electric field can potentially change SPP characteristics.

We consider the geometry shown in Fig. 1(a) of two parallel semi-infinite ferroelectric materials separated by a distance d, kept at temperatures T_1 and T_2, and with applied electric fields E_1 and E_2 respectively. The radiative heat exchange for this geometry can be calculated via fluctuating electrodynamics method established by Rytov and Polder et al. [1 – 2, 6 - 11]. The approach is based

on the solution of Maxwell equations via the fluctuation-dissipation theorem with the thermally excited electron fluctuations inside the materials as the sources of electromagnetic radiation. The total heat flux across the gap between two surfaces is calculated as the difference between the Poynting fluxes originated from the hot and cold sides. For isotropic and nonmagnetic materials with constant optical properties, the expression for thermal radiation between two parallel semi-infinite materials reads as [1 - 2, 6 – 11]

$$P(T_1,T_2,d) = \int_0^\infty d\omega \left[\Theta(\omega,T_1) - \Theta(\omega,T_2)\right] f(\omega;d) \tag{1}$$

where $\Theta(\omega,T) = \hbar\omega[\exp(\hbar\omega/k_BT)-1]^{-1}$ is the average energy of a photon with angular frequency ω emitted from a source at equilibrium temperature T, and $f(\omega;d)$ is the spectral transmission function [11]. The average photon energy depends only on the surface temperature, but the transmission function f(ω;d) depends strongly on the surface optical properties [6 – 11]. In the case of far-field blackbody emitters and absorbers, the dominant wavelength of thermal radiation is determined by the difference in photon energy emitted from hot and cold side ($\Theta(T_1) - \Theta(T_2)$), and can be approximated by the Wien's law ($\lambda T_{avg} \sim 3000\mu mK$) where T_{avg} is the mean temperature of hot and cold sides. In the near-field regime, thermal radiation is also excited according to ($\Theta(T_1) - \Theta(T_2)$) as evident in Eq. (1), but the spectrum is further shaped by the spectral transmission function f(ω; d).

The spectral transmission function describes the probability for a photon with frequency ω to transport through the gap, and for each frequency it is integrated over all the photon momenta parallel to the interfaces (i.e. over parallel wave vectors k_p) so that all modes are accounted for. It takes into account reflection and absorption of photons, as well as interference of both evanescent and propagating waves within the gap. The contribution to the total near-field heat flux that is due to

near-field coupling of evanescent waves for either TE or TM polarization is given as [6-11]

$$f(\omega;d,T_1,T_2,E_1,E_2)=\frac{1}{\pi^2}\int_{k_p=\omega/c}^{\infty}k_p\,dk_p\exp(-2k_z''d)\left[\frac{\mathrm{Im}(r_1(T_1,E_1))\mathrm{Im}(r_2(T_2,E_2))}{\left|1-r_1(T_1,E_1)r_2(T_2,E_2)\exp(-2ik_z''d)\right|^2}\right] \quad (2)$$

where r_1 (r_2) is the Fresnel reflection coefficient for photons incident from material 1(2) at the interface with the surrounding medium 0 for either TE or TM polarization, k is the total wave vector, k_p is the wavevector parallel to the interface, and k_z'' is the imaginary part of the perpendicular wave vector $k_z = (k^2 - k_p^2)^{1/2}$. Due to temperature and electric-field dependent optical properties of ferroelectric materials, Fresnel reflection coefficients $r_{1(2)}$ both depend on the temperature $T_{1(2)}$ and external electric field $E_{1(2)}$. At frequencies corresponding to the excitation of the surface phonon polaritons, the transmission function exhibits strong resonances. These reflect the resonant enhancement of the density of photon states associated with the flat dispersion characteristics of surface modes, which include high-momenta photon states [3, 4, 8, 10, 14, 15, 33].

We assume a specific type of material, $SrTiO_3/DyScO_3$ superlattice grown on $DyScO_3$ substrate, where only $SrTiO_3$ is ferroelectric and $DyScO_3$ is not ferroelectric. The phase change temperature, or Curie temperature of this ferroelectric film is around 280K [34 - 36]. The dielectric property of the superlattice is approximated by effective medium theory, and we use experimental data of the materials fitted with temperature-dependent and electric-field dependent parameters from Reference 34. We note that bulk ferroelectric materials of pervoskite structure, such as $SrTiO_3$, have also been experimentally verified to exhibit tunable TO phonon frequencies [32].

The dielectric function near the tunable TO frequency can be described by Lorentz-model [12, 34 - 36], which models the resonant interaction of optical phonons and photons, whereas at low frequencies, the Debye model [12, 34 - 36] accounts for delayed alignment of permanent dipoles in the perovskite

structure with the electric field. Figure 1(b) shows the real part of the material dielectric constant at different temperatures and for different applied dc electric fields. When the material is in ferroelectric phase, increasing temperature increases the static dielectric constant and lowers the tunable TO frequency according to the Lydanne-Sachs-Teller relation [12]. In the material studied, increasing applied electric field increases the tunable TO frequency. We do not comment on the origin of phonon hardening since it is not the focus of this paper [37, 38].

One can calculate the spectral heat flux and total heat flux using Eqs. (1) and (2) by plugging in the dielectric spectrum in Fig. 1(b). We assume that applied electric fields on the hot side with temperature T_1 and cold side with temperature T_2 are E_1 and E_2, respectively. Figure 2(a) shows the transmission function for the case T_1 = 20K and T_2 = 80K with zero external dc fields ($E_1 = E_2$ = 0kV/cm) and a gap width d of 100nm. It should be noted that dielectric constants of ferroelectric materials could still be tuned even at temperatures that are far away from the transition temperature [34 – 38]. High momenta modes near 2THz and 5THz observed in Fig. 2 are coupled SPP modes, which are excited owing to resonant interaction of photons with optical phonons of the material. The narrow bandwidths of these two SPPs-coupling-induced peaks distinguish them from the broad spectrum of blackbody radiation. There exist two high momenta modes because the real part of the material permittivity becomes negative in the spectral range around the tunable TO frequency, which creates conditions for the excitation of two surface phonon polariton modes with close frequencies at the ferroelectric-vacuum interface.

Figure 2(b) and 2(c) demonstrate how the frequency spectrum of the radiative heat flux changes when the applied external electric fields are varied, whereas the separation distance is fixed at 100nm and temperatures are fixed at T_1 = 20K and T_2 = 80K. In Fig. 2(b), we compare the spectral heat flux without applied electric field and spectral heat flux with 80kV/cm electric field applied on both hot and

cold sides. The SPP-mediated heat transfer is significantly enhanced over the conventional case of the blackbody thermal emitter and absorber, which is shown for comparison as the black line. As exhibited in Fig 2(a), the two peaks in the transmission function shown in Figs. 2b,c correspond to tunneling of SPP waves across the narrow gap between two surfaces. As applied electric fields increase the tunable TO frequency, the peaks corresponding to SPPs blueshift by around 500 THz. This demonstrates that frequencies of the dominant near-field thermal radiation can be electrically tuned.

As seen in Fig. 2(c), magnitudes of spectral heat transfer peaks can be modulated by varying the external electric fields independently on the hot and cold sides. When both sides support surface phonon polaritons at similar frequencies, coupling between surface phonon polaritons is enhanced, thus increasing the values of the transmission function $f(\omega;k)$ in Eq. 2 [11, 33]. Without external electric field, the first TO frequency on material 2 is higher than that at material 1 since $T_2 > T_1$. The application of the electric field on side 1 (i.e. E_1 = 80kV/cm, E_2 = 0) increases its TO frequency and provides a better overlap of the TO frequencies on the opposing sides, which in turn increases the radiative heat flux as compared to the zero external field case. Applying electric field on side 2 (i.e. E_1 = 0, E_2 = 80kV/cm), however, pushes the TO frequencies supported on two sides further apart and thus decreases the radiative heat flux.

Total heat transfer from the hot to the cold surface across the gap can be found by integrating the heat transfer spectrum in Fig. 2 over the whole frequency range. We find that by applying electric field only, the total heat flux can be changed by as much as 16.5% when temperatures are fixed at T_1 = 20K and T_2 = 80K and the gap is fixed at 100nm. Figure 3 demonstrates how the total heat flux can be changed by applying external dc electric fields. The electric field values are cut off at 80kV/cm since the material breaks down at such field magnitude. The total heat flux is monotonically increasing with hot-side applied electric field, which, as discussed above, brings the frequencies of SPP modes on the

opposite sides of the gap closer. We also notice that since the integrated heat flux does not exhibit a local maximum, one can further increase total heat flux by bringing the SPP frequencies on hot and cold surfaces closer and increasing the coupling between the SPP modes, as long as the electric field is smaller than the breakdown field.

We can further define the tunability of total heat flux by external electric field as $T(\%) = (q_{max} - q_{min})/q_{min}$. As evident in Fig. 3, q_{max} is 152.23 W/m^2 and q_{min} is 130.43 W/m^2, and the tunability at this configuration (i.e. T_1 = 20K, T_2 = 80K, d = 100nm) is 16.5%. Figure 4(a) shows the tunability of total heat flux due to varying only the external electric fields for different temperature combinations. The largest change in total heat flux is around T_1 = 20K and T_2 = 80K, which corresponds to the cases shown in Fig. 4(a). It is not surprising that the largest change in heat flux happens near these temperatures, because in this case the dominant wavelengths of thermal radiation determined by $(\Theta(T_1) - \Theta(T_2))$ match closely with the SPP wavelengths. The first TO mode has vacuum wavelengths between 50 - 100μm and thus largest tunability of heat flux happens around temperature ranges of 30-60K. Figure 4(b) plots the enhancement of radiative heat flux over blackbody radiation with varying temperatures T_1 and T_2. Similar to Fig. 4(a), the maximum enhancement over blackbody happens near temperatures when dominant wavelengths of thermal emission correspond to SPP frequencies, since tunneling of SPPs across the gap is a major contributor to enhanced radiation in the near-field regime. The minimum and maximum temperatures represented are 20K and 315K, since dielectric constants of the material have not been measured at temperatures outside 20K – 315K [34].

In summary, we predict via rigorous numerical analysis the possibility of dynamically tuning the intensity, the frequency spectrum and the total thermal emission exchange between ferroelectric surfaces. The maximum modulation of total radiative heat flux for our specific material system can be 16.5% using externally applied electric field at T_1 = 20K and T_2 = 80K temperatures. The maximum

spectrum shift of radiation is on the order of 1THz at the same temperatures. Our simulation results suggest that ferroelectrics can be used to develop new types of tunable nanoscale devices for thermal and energy conversion applications. Although demonstrated in the low temperature regime, this mechanism can also be used to achieve thermal emission tunability at higher temperatures (and thus in a higher photon frequency ranges). In particular, to achieve electrical tunability at the room temperature, the TO frequency of materials needs to correspond to wavelength of 10um, which is about 5 times higher than that of the current material. Therefore, the room-temperature applications may be possible by using lighter-mass and stiffer ferroelectric-like materials [12]. The experimental feasibility of a room-temperature device based on the proposed mechanism needs to be further explored.

Acknowledgements

The authors acknowledge funding support from DOE BES (DE-FG02-02ER45977). The authors would like to thank Sangyeop Lee for providing initial inspiration and advice on the properties of ferroelectric materials, Poetro L. Sambegoro, Jonathan K. Tong, Vazrik Chiloyan, Wei-Chun Hsu, and Dr. Selcuk Yerci for useful discussions.

References

[1] D. Polder and M. Van Hove, “Theory of Radiative Heat Transfer between Closely Spaced Bodies,” *Phys. Rev. B*, vol. 4, no. 10, pp. 3303–3314, Nov. 1971.

[2] S. M. Rytov, “Theory of Electric Fluctuations and Thermal Radiation,” *Air Force Cambridge Research Center*, Bedford, MA, 1959.

[3] S. Shen, A. Narayanaswamy, and G. Chen, “Surface phonon polaritons mediated energy transfer between nanoscale gaps.,” *Nano Lett.*, vol. 9, no. 8, pp. 2909–13, Aug. 2009.

[4] L. Hu, A. Narayanaswamy, X. Y. Chen, and G. Chen, “Near-field thermal radiation between two closely spaced glass plates exceeding Planck’s blackbody radiation law”, *Applied Physics Lett*ers

vol. 92, no. 13, pp. 133106, Apr. 2008.

[5] E. Rousseau, A. Siria, G. Jourdan, S. Volz, F. Comin, J. Chevrier, J. -J. Greffet, "Radiative Heat Transfer at the Nanoscale", *Nature Photonics*, v. 3, pp. 514-517, Sept. 2009.

[6] A. Narayanaswamy and G. Chen, "Direct computation of thermal emission from nanostructures", *Annual Review of Heat Transfer*, vol. 14, no. 130, pp. 169-195, 2005.

[7] A. Narayanawamy, S. Shen, and G. Chen, "Near-field Radiative Transfer Between a Sphere and a Substrate," *Physical Review B*, vol. 78, no. 11, pp. 115304, Sept. 2008.

[8] A. Narayanaswamy, S. Shen, L. Hu, X. Y. Chen, and G. Chen, "Breakdown of the Planck blackbody radiation law at nanoscale gaps," *Appl. Phys. A*, vol. 96, no. 2, pp. 357–362, May 2009.

[9] J.-P. Mulet, K. Joulain, R. Carminati, and J.-J. Greffet, "Enhanced radiative heat transfer at nanometric distances," *Microscale Thermophysical Engineering*, vol. 6. pp. 209–222, 2002.

[10] A. Shchegrov, K. Joulain, R. Carminati, and J. -J. Greffet, "Near-field Spectral Effects due to Electromagnetic Surface Excitations," *Physical Review Letters*, vol. 85, pp.1548- 1551, Aug. 2000.

[11] M. Francoeur, M. P. Mengüç, and R. Vaillon, "Solution of near-field thermal radiation in one-dimensional layered media using dyadic Green's functions and the scattering matrix method," *Journal of Quantitative Spectroscopy & Radiative Transfer,* vol. 110, no. 18, pp. 2002 – 2018, May 2009.

[12] N. W. Ashcroft and N. D. Mermin, "Solid State Physics," 1976.

[13] A. Narayanaswamy, and G. Chen, "Thermal Radiation Control with 1D Metallo-Dielectric Photonic Crystals," *Physical Review B,* vol. 70, no. 12, pp. 125101, Sept. 2004.

[14] P. Ben-Abdallah, K. Joulain, J. Drevellion, and G. Domingues, "Near-Field Heat Transfer Mediated by Surface Wave Hybridization between Two Films," *Journal of Applied Physics*, vol. 106, pp. 044306, Aug. 2009.

[15] M. Francoeur, M. P. Menguc, and R. Vaillon, "Control of near-field radiative heat transfer via surface phonon-polariton coupling in thin films," *Appl. Phys. A. Mater. Sci. Proces.*, vol. 103, no. 3, pp. 547–550, Jan. 2011.

[16] J. P. Mulet, K. Joulain, R. Carminati, and J. –J. Greffet, "Nanoscale Radiative heat Transfer between A Small Particle and a Plane Surface," *Applied Physics Letters*, Vol. 78, pp. 2931-2933, Mar. 2001.

[17] A. Narayanaswamy, and G. Chen, "Thermal Near-field Radiative Transfer between Two Spheres," *Physical Review B*, Vol. 77, p. 075125, Feb. 2008.

[18] S.-A. Biehs, F. S. S. Rosa, and P. Ben-Abdallah, "Modulation of near-field heat transfer between two gratings," *Applied Physics Letters*, vol. *98*, no. 24, pp. 243102, June 2011.

[19] L. Zhu, C. R. Otey, and S. Fan, "Ultrahigh-contrast and large-bandwidth thermal rectification in near-field electromagnetic thermal transfer between nanoparticles," *Physical Review B*, vol. *88*,

no. 18, pp.184301, Nov. 2013.

[20] P. J. van Zwol, K. Joulain, P. Ben-Abdallah, and J. Chevrier, "Phonon polaritons enhance near-field thermal transfer across the phase transition of VO_2," *Physical Review B*, vol. 84, no. 16, p. 161413, Oct. 2011.

[21] C. R. Otey, W. T. Lau, and S. Fan, "Thermal Rectification through Vacuum," *Physical Review Letters,* vol. 104, p. 154301, Apr. 2010.

[22] P. Ben-Abdallah, and S. -A. Biehs, "*Phase-change radiative thermal diode," Applied Physics Letters,* vol. 103, no. 19, pp. 191907, Nov. 2013.

[23] Y. Yang, S. Basu, and L. Wang, "*Radiation-based near-field thermal rectification with phase transition materials"*, *Applied Physics Letters,* vol. 103, no. 16, pp. 163101, Oct. 2013.

[24] E. Nefzaoui, K. Joulain, J. Drevillon, and Y. Ezzahri, "Radiative thermal rectification using superconducting materials", *Applied Physics Letters,* vol. 104, no. 10, pp. 103905, Mar. 2014.

[25] S. Basu and M. Francoeur, "Near-field radiative transfer based thermal rectification using doped silicon," *Appl. Phys. Lett.*, vol. 98, no. 11, p. 3, Mar. 2011.

[26] J. Shi, P. Li, B. Liu, and S. Shen, "Tuning near field radiation by doped silicon," *Applied Physics Letters*, vol. 102, no. 18, p. 183114, May 2013.

[27] O. Ilic, M. Jablan, J. D. Joannopoulos, I. Celanovic, H. Buljan, and M. Soljačić, "Near-field thermal radiation transfer controlled by plasmons in graphene,"*Physical Review B*, vol. 85, no. 15, p. 155422, Apr. 2012.

[28] R. Messina, J. P. Hugonin, J. -J. Greffet, F. Marquier, Y. De Wilde, A. Belarouci, L. Frechette, Y. Cordier, and P. Ben-Abdallah, P, "Tuning the electromagnetic local density of states in graphene-covered systems via strong coupling with graphene plasmons," *Physical Review B*, vol. 87, no. 8, p. 085421, Feb. 2013.

[29] T. Inoue, M. De Zoysa, T. Asano, and S. Noda, "Realization of dynamic thermal emission control," *Nature Materials*, vol. 13, no. 10, p. 928-931, July 2014.

[30] L. Cui, Y. Huang, J. Wang, and K. Y. Zhu, "Ultrafast modulation of near-field heat transfer with tunable metamaterials", *Applied Physics Letters*, vol. 102, no. 5, pp. 053106, Feb. 2013.

[31] J. H. Haeni, P. Irvin, W. Chang, R. Uecker, P. Reiche, Y. L. Li, S. Choudhury, W. Tian, M. E. Hawley, B. Craigo, A. K. Tagantsev, X. Q. Pan, S. K. Streiffer, L. Q. Chen, S. W. Kirchoefer, J. Levy and D. G. Schlom, "Room-temperature ferroelectricity in strained $SrTiO_3$," *Nature*, vol. 430, no. 7001, p. 758-761, Aug. 2004.

[32] P. A. Fleury, and J. M. Worlock, "Electric-Field-Induced Raman Scattering in $SrTiO_3$ and $KTaO_3$," *Physical Review*, vol. 174, no. 2, p. 613, Oct. 1968.

[33] S. V. Boriskina, H. Ghasemi, and G. Chen, "Plasmonic materials for energy: From physics to applications," *Materials Today*, vol. 16, no. 10, p. 375-386, Oct. 2013.

[34] C. Kadlec, V. Skoromets, F. Kadlec, H. Němec, J. Hlinka, J. Schubert, G. Panaitov, and P. Kužel, "Temperature and electric field tuning of the ferroelectric soft mode in a strained $SrTiO_3/DyScO_3$ heterostructure," *Physical Review B*, vol. 80, no. 17, p. 174116, Nov. 2009.

[35] P. Kuzel, F. Kadlec, J. Petzelt, J. Schubert, and G. Panaitov, "Highly tunable $SrTiO_3/DyScO_3$ heterostructures for applications in the terahertz range," *Applied Physics Letters*, vol. 91, no. 23, pp. 232911-232911, Dec. 2007.

[36] P. Kužel, C. Kadlec, F. Kadlec, J. Schubert, and G. Panaitov, "Field-induced soft mode hardening in SrTiO3/DyScO3 multilayers," *Applied Physics Letters*, vol. 93, no. 5, pp. 052910, Aug. 2008.

[37] I. A. Akimov, A. A. Sirenko, A. M. Clark, J. H. Hao, and X. X. Xi, "Electric-Field-Induced Soft-Mode Hardening in $SrTiO_3$ Films," *Physical Review Letters*, vol. 84, no. 20, pp. 4625, May 2000.

[38] A. A. Sirenko, C. Bernhard, A. Golnik, A. M. Clark, J. H. Hao, W. Si, and X. X. Xi, "Soft-mode hardening in $SrTiO_3$ thin films", *Nature*, vol. 404, no. 6776, pp. 373-376, Mar. 2000.

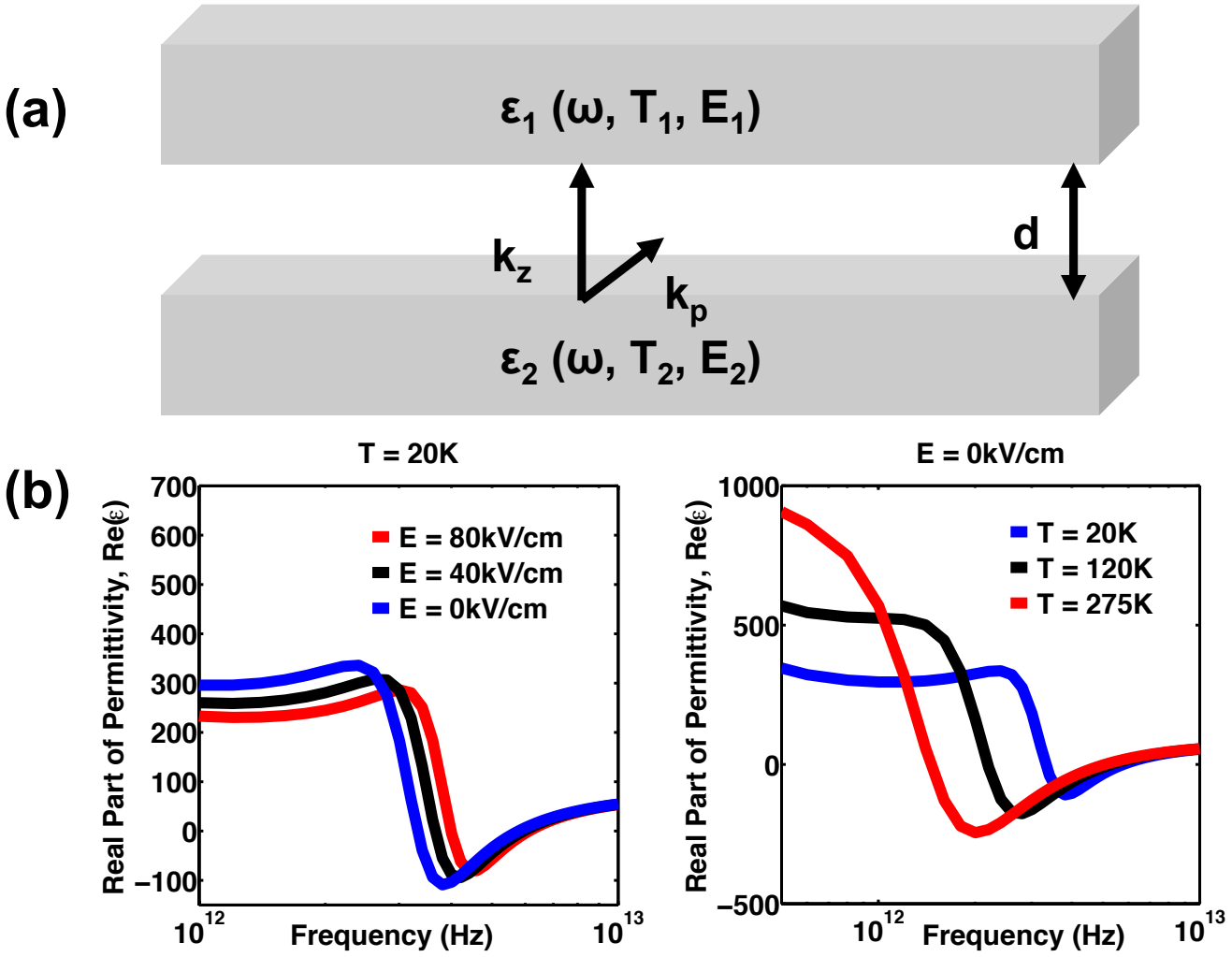

Figure 1: (a) Schematic diagram showing configuration of radiative heat transfer, and (b) real part of dielectric constant of ferroelectric materials in Reference [34] at different temperatures (T = 20K, 120K and 275K respectively with no applied electric field) and at different electric fields (E = 0, 40 and 80 kV/cm respectively at T = 20K).

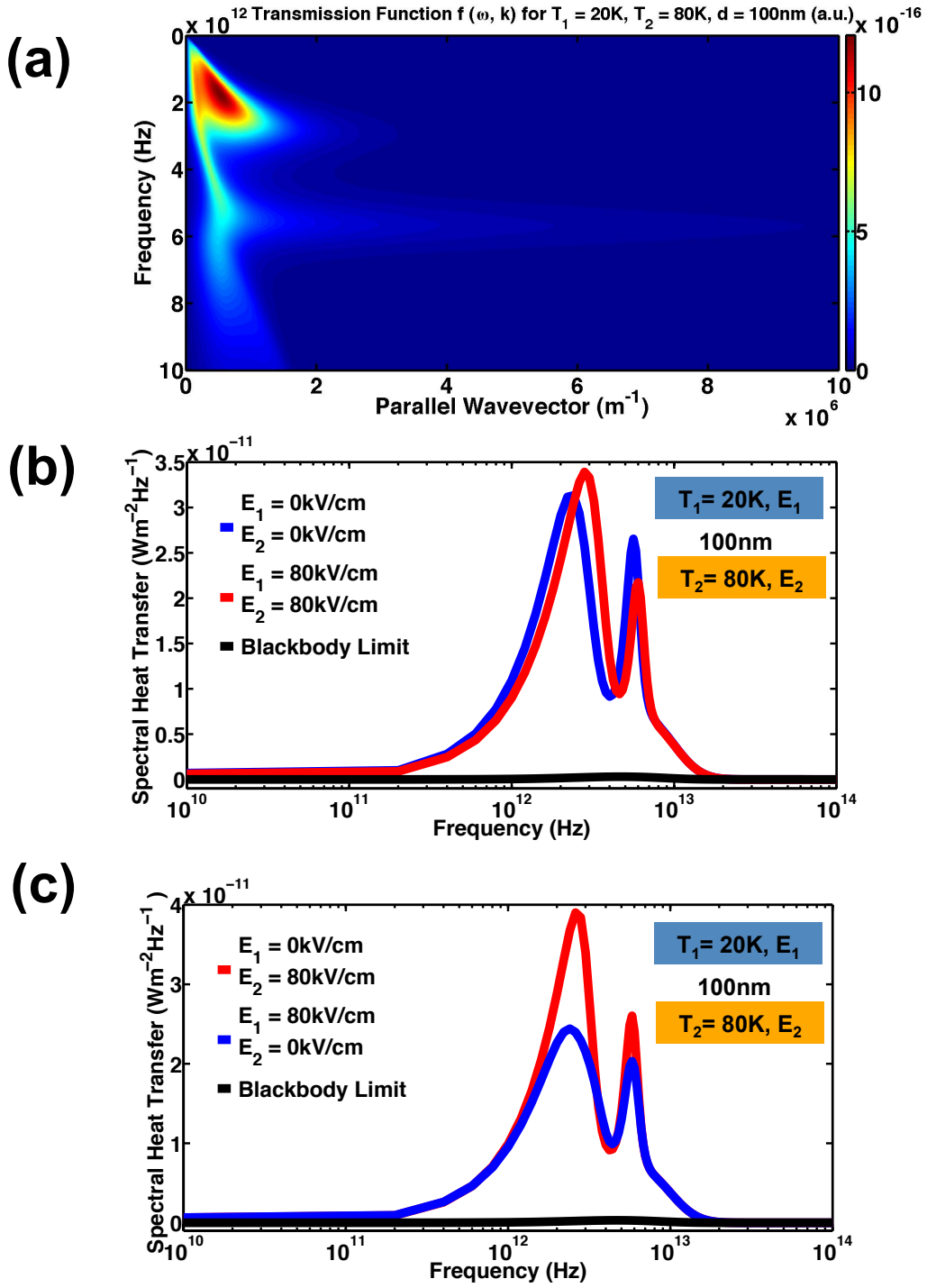

Figure 2: Radiative heat flux between simulated ferroelectric materials when T_1 = 20K and T_2 = 80K at a separation distance of 100nm between hot and cold surfaces. (a) Transmission function f(ω,k) as a function of frequency ω and parallel wavevector k_ρ. (b) Shift in the heat flux spectrum using external electric field (blue: E_1 = 0kV/cm, E_2 = 0kV/cm; red: E_1 = 80kV/cm, E_2 = 80kV/cm). (c) Magnitude of spectral heat flux is modulated via external electric field (blue: E_1 = 0kV/cm, E_2 = 80kV/cm; red: E_1 = 80kV/cm, E_2 = 0kV/cm).

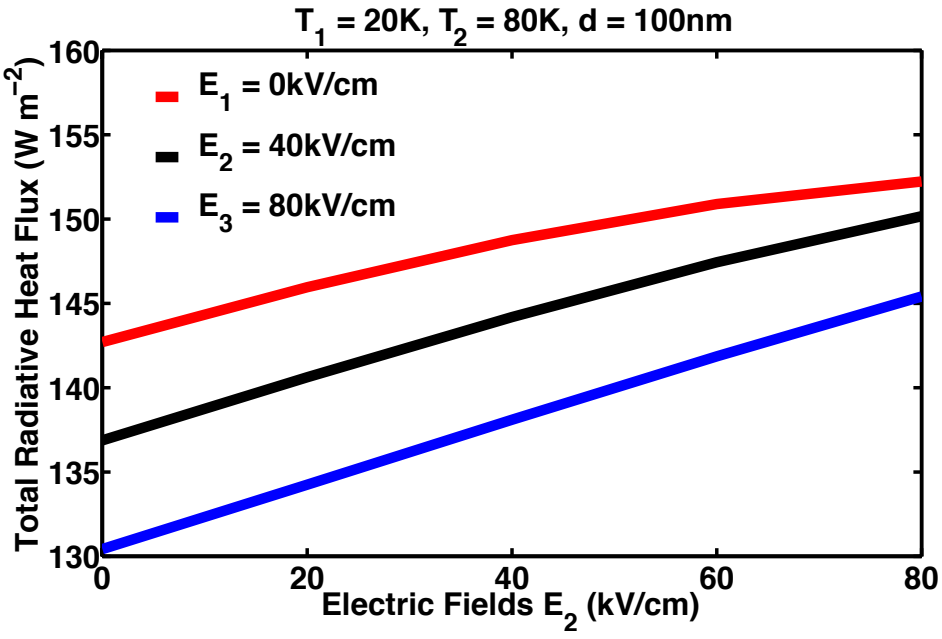

Figure 3. Tunability of the total heat flux between abovementioned ferroelectric materials with varying external electric field. All calculations are for temperatures T_1 = 20K and T_2 = 80K and a gap size of 100nm.

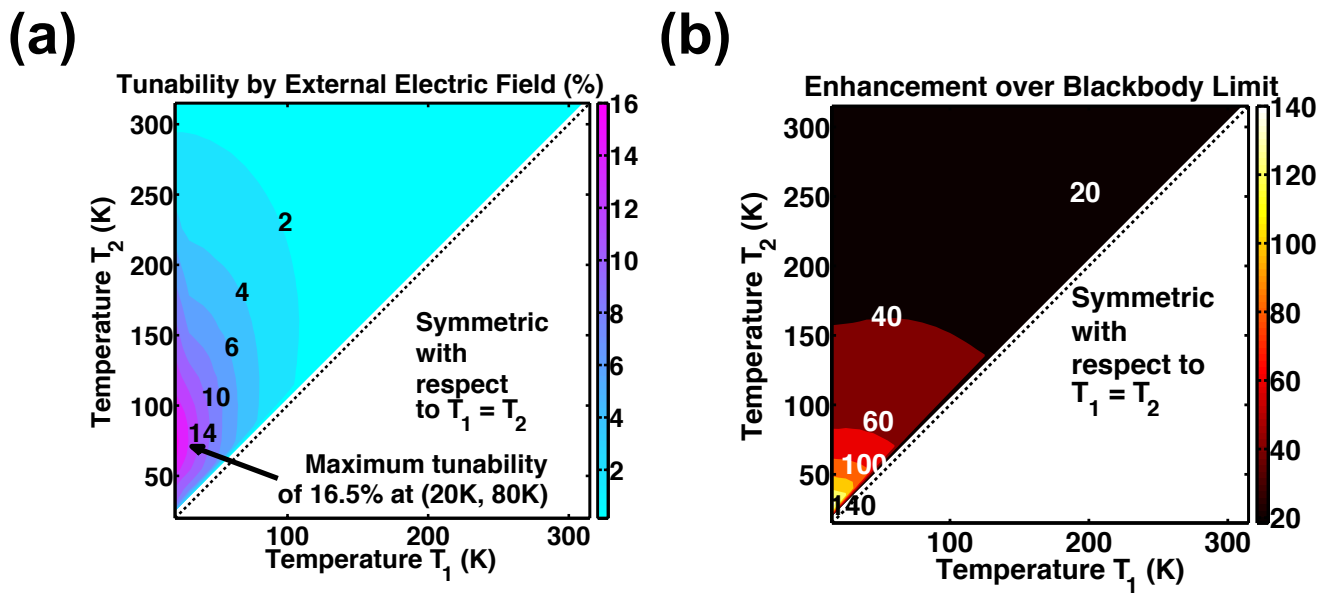

Figure 4: (a) Tunability of total heat flux using external electric fields only at different temperature combinations for temperatures ranging from 20K to 315K at separation distance of 100nm between hot and cold sides. (b) Enhancement of radiative heat flux over blackbody radiation limit at different temperature combinations for temperatures ranging from 20K to 315K at separation distance of 100nm between hot and cold sides. Both plots are symmetric along the dashed line $T_1 = T_2$.